Cancer Chemother Pharmacol (1996) 39: 122–130 

ORIGINAL ARTICLE

**Ahmed E. Ahmed · Sam Jacob · Beppino C. Giovanella**
**Anthony J. Kozielski · John S. Stehlin, Jr.**
**Joachim G. Liehr**

# Influence of route of administration on [$^3$H]-camptothecin distribution and tumor uptake in CASE-bearing nude mice: whole-body autoradiographic studies

Received: 13 May1994/Accepted: 18 March 1996

**Abstract** Camptothecin (CPT) inhibits the growth of a wide variety of experimental tumors. As a part of our exploration of this drug for use as a cancer chemotherapeutic agent, we studied the effect of route of administration on the absorption, distribution and tumor uptake of [$^3$H]-CPT. The rate of disappearance of [$^3$H]-CPT-derived radioactivity from blood during the first 48 h was highest following oral than following intravenous (i.v.) administration. Thereafter blood levels were low irrespective of route of administration. Considerable [$^3$H]-CPT-derived radioactivity was detected in urine and feces up to 48 h after dosing. Distribution studies were conducted using quantitative whole-body autoradiography (WBA). These studies revealed that independent of the route of administration, [$^3$H]-CPT was rapidly excreted in the bile (gallbladder) followed by elimination into the small and large intestinal tract. Levels of CPT-derived radioactivity in the kidneys were minimal and mostly localized in the renal pelvis. Hepatic concentrations of CPT were low and were almost equal to those of the tumor. The lungs of animals treated i.v. showed higher uptake of radioactivity than those treated intramuscularly or orally. Tumor/blood ratios were slightly higher following oral administration than following administration by other routes. This study indicates that CPT is primarily eliminated via the bile. The gastrointestinal tract is the major site of accumulation and excretion of CPT.

**Key words** Camptothecin · Whole-body autoradiography · Tumor uptake · CASE

A.E. Ahmed (✉) · S. Jacob
Departments of Pathology and Cancer Center,
The University of Texas Medical Branch, Galveston,
TX 77555-0609, USA
Tel. (409) 772-2877; Fax. (409) 747-2429

B.C. Giovanella · A.J. Kozielski · J.S. Stehlin, Jr.
Stehlin Foundation for Cancer Research, Houston,
TX 77002, USA

J.G. Liehr
Department of Pharmacology and Toxicology,
The University of Texas Medical Branch, Galveston,
TX 77555-0605, USA

## Introduction

The plant alkaloid camptothecin (CPT), and its structural analogues inhibit the growth of a variety of tumors [9, 15, 18] including murine leukemia [1]. Previous reports suggest impressive antitumor activity of CPT in human tumors (colon, breast, lung) xenografted in nude mice [7, 13]. Recent studies on the mechanism of CPT anticancer action have indicated that its activity is attributable to its inhibition of DNA topoisomerase I [4, 6, 12, 19].

The biologic fate and toxicity of CPT and several of its structural analogues have also been examined [14, 22, 23, 24]. Guarino et al. have demonstrated biliary and urinary excretion to be the major routes of elimination when CPT is administered intraperitoneally (i.p.) [16]. The influence of route of administration upon excretion and relative organ/tumor uptake of CPT in an intact animal model have not been studied. Because of the clinical importance of CPT and its analogues, an understanding of the metabolism and compartmental kinetics of this drug (CPT) is essential for the enhancement of its pharmacological effectiveness. Whole-body autoradiography (WBA) combined with image analysis provides comprehensive information on the inter- and intraorgan distribution pattern of the drug in all tissues including that of the tumor without any alteration of the blood flow [3]. Hence, the objective of this study was to use WBA to investigate the differential disposition of CPT following various routes of administration in nude mice bearing human colon carcinoma (CASE) to characterize the effect of route of administration on the biologic fate and tumor uptake of the drug.

## Materials and methods

### Chemicals

CPT was purchased from Good Land Enterprises, Vancouver, B.C., Canada. Uniformly [$^3$H] -labeled CPT was purchased from American Radiochemicals, St. Louis, Mo. Its purity (96%) was determined in our laboratory by high-performance reversed-phase liquid chromatography [20]. The specific activity of the purified [$^3$H]-CPT was 1.5 mCi/μmol. The stability of the radiolabeled CPT was examined in other studies [17]. Tritium loss from this preparation occurs in vivo and in vitro with a half-life of 16.5 h [17]. Acetonitrile (HPLC grade) was obtained from Fisher Scientific (Pittsburgh, Pa.). Carbsorb II and Permafluor were obtained from the Packard Instrument Company (Laguna Hills, Calif.). Aquasol-2 was purchased from New England Nuclear Research Products (Boston, Mass.). The specific activity of the dosing solution was determined in PCS Scintillation Fluor (Amersham, Chicago, Ill.) using a Beckman (Fullerton, Calif.) LS 7500 scintillation counter. Counting efficiency was determined using external standardization. All other chemicals and reagents used in these studies were of the highest purity commercially available.

### Animals and tumor implantation

Swiss immunodeficient (nude) mice (weighing 30–35 g) of the NIH-1 high fertility strain were bred and maintained under strict pathogen-free conditions in our laboratory and were used for these experiments [10]. Animals were inoculated with CASE [11]. This tumor is totally resistant to most conventional anticancer drugs [25], but is sensitive to CPT and its derivatives [27, 28]. Human malignant tumors were transplanted into mice by inoculating 50 mg of finely minced tumor tissue in 0.5 ml Eagle's minimum essential medium (GIBCO, Long Island, N.Y.) under the skin of the dorsal chest region. [$^3$H] -CPT treatment was started 8 days after inoculation when tumors had grown to a size of approximately 1.0 cm diameter.

### Animal treatment

To ensure the comparability of our data, a fine microsuspension/microemulsion of [$^3$H]-CPT in Intralipid 20 (Kabil Vitrum, Alameda, Calif.) was used for all routes of administration. This suspension was administered intravenously (i.v.) into the tail vein or intramuscularly (i.m.) into the femoral muscle of tumor-bearing mice (0.1 ml/mouse) . This volume has previously been shown to be well tolerated and to cause no apparent ill-effects to treated animals. To avoid intragastric toxicity, the [$^3$H] -CPT suspension was mixed with a paste consisting of 1 g of whole-wheat bread saturated with milk. This paste was administered orally to fasted mice prior to daily food rations to assure rapid and complete consumption. Each mouse received 4 mg/kg CPT with an activity 300 μCi/kg independent of the route of administration. Treated animals were placed in all-glass metabolism cages throughout the experiment.

### Collection of plasma, urine and feces

Plasma was collected at various time intervals following treatment with [$^3$H]-CPT by different routes of administration. For the collection of plasma, mice (3–5 animals/group) were treated i.v. with a heparin solution and blood was collected by cardiac puncture under anesthesia. Red and white blood cells and plasma were separated by centrifugation at 2000 g for 10 min at room temperature. The plasma was stored frozen (− 70 °C) until its radioactivity was determined. For radioactivity determination, plasma (25 μl) was mixed with 10 ml of Ready-Gel (Beckman Instruments, Fullerton, Calif.) and radioactivity contents were determined using a scintillation counter (LS 7500, Beckman Instruments). Urine and feces were collected separately in metabolism cages at 24-h intervals up to 120 h following treatment with the drug. Aliquots of the urine were mixed with scintillant and counted. Feces were homogenized in Protosol, treated with hydrogen peroxide, dissolved in scintillant and counted.

### Whole-body autoradiography

WBA was carried out by a modification of Ullberg's method [3] Briefly, treated animals (3–5 mice/group) were sacrificed by $CO_2$ anoxia 30 min, 2 h and 12 h after [$^3$H]-CPT administration. Carcasses were immediately flash frozen by immersion in a mixture of hexane and dry ice at − 70 °C for about 5 min. Frozen carcasses were embedded in carboxymethyl cellulose gel. The gel containing the carcass was again immersed in a mixture of hexane and dry ice at − 70 °C for 15 min and stored at − 20 °C until the time of sectioning. Multiple sagittal sections of 30 μm thickness were then cut with a cryomicrotome (LKB PMV 2250) maintained at − 20 °C. Animal sections in which several organs could easily be identified were mounted on Scotch tape 800 (3 M Co. St. Paul, Minn.). For autoradiography, Amersham Ultra film (Amersham Industries, Chicago, Ill.) was placed on the mounted animal sections along with precalibrated 30 μm [$^3$H] reference strips (Microscales, Amersham, Chicago, Ill.) and processed at different exposure times ranging from 5 to 8 weeks, to compensate for the saturation of radioactivity on the film.

Representative autoradiographs were used as negatives for the production of photographs (Figs. 1–3). Therefore, in the figures presented, white areas represent sites of high radioactivity uptake. The gray to back intensities represent sites of medium to low levels of radioactivity. Complementary determinations of the total radioactivity content in various organs were carried out by dissolving aliquots of tissues in Protosol and counting as described above.

### Computer-assisted image analysis of WBA

The distribution pattern of [$^3$H]-CPT was determined using computer-assisted image analysis of the autoradiographs [2]. Autoradiographs were selected from three mice per time-point and route of administration. In each autoradiograph, the maximum number of organs anatomically identifiable were studied in detail. Several samples representing different areas of an organ were picked from these autoradiographs to evaluate the intraorgan distribution of radioactivity. Optical densities for different organs in these autoradiographs were determined with an autoscanning image analyzer (MCID), manufactured by Imaging Research, Brock University, (St. Catherine, Canada). Briefly, a response curve relating the level of activity to a digitized number (an arbitrary number produced by the video camera) was constructed by digitizing a step-wise series of autoradiographed radioisotopic standards. The computer used this information to calculate the actual amount of radioactivity in each pixel of the digitized matrix. The final step in calculating the levels of activity in each pixel of the digitized image involved performing a polynomial fitting to the standard calibration curve or by linear regression analysis. The quantified image was then displayed by coding 16 different levels of activity. Regions of interest were then selected by using the MCID System to analyze the autoradiographs. Ten or more pixels from each region or tissue were sampled, digitized, and converted to nanocuries per gram of tissue using the calibrated autoradiographic standard curve. From these values, the means and standard deviations were calculated. Total blood values were determined in cardiac cavities and/or abdominal aorta.

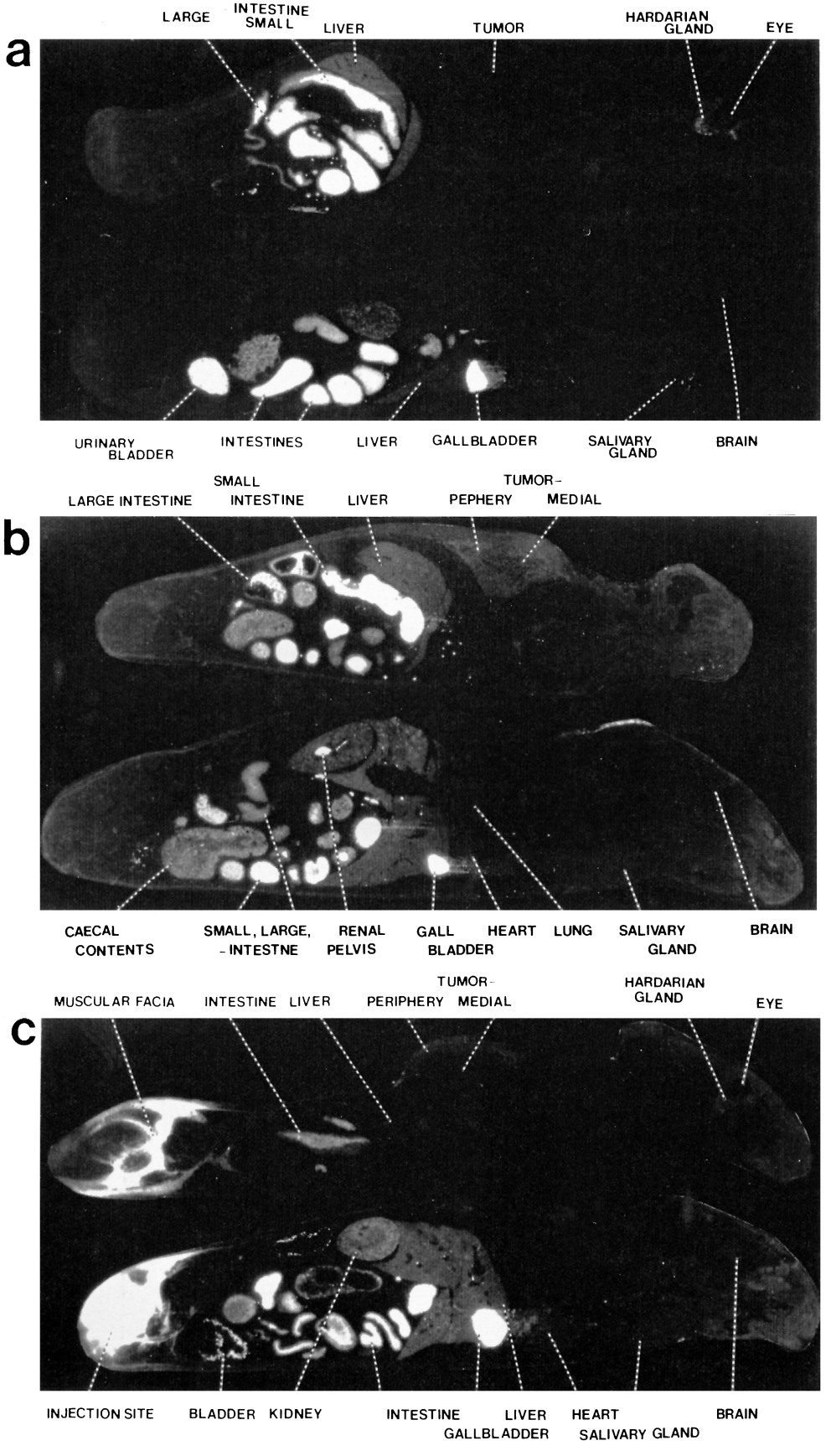


**Fig. 1 a–c** Whole body autoradiograms of mice at 30 min following (**a**) oral, (**b**) i.v. and (**c**) i.m. administration of [$^3$H]-CPT (300 μCi/kg). Irrespective of route of administration, rapid uptake of radioactivity can be seen in the intestinal contents and gallbladder

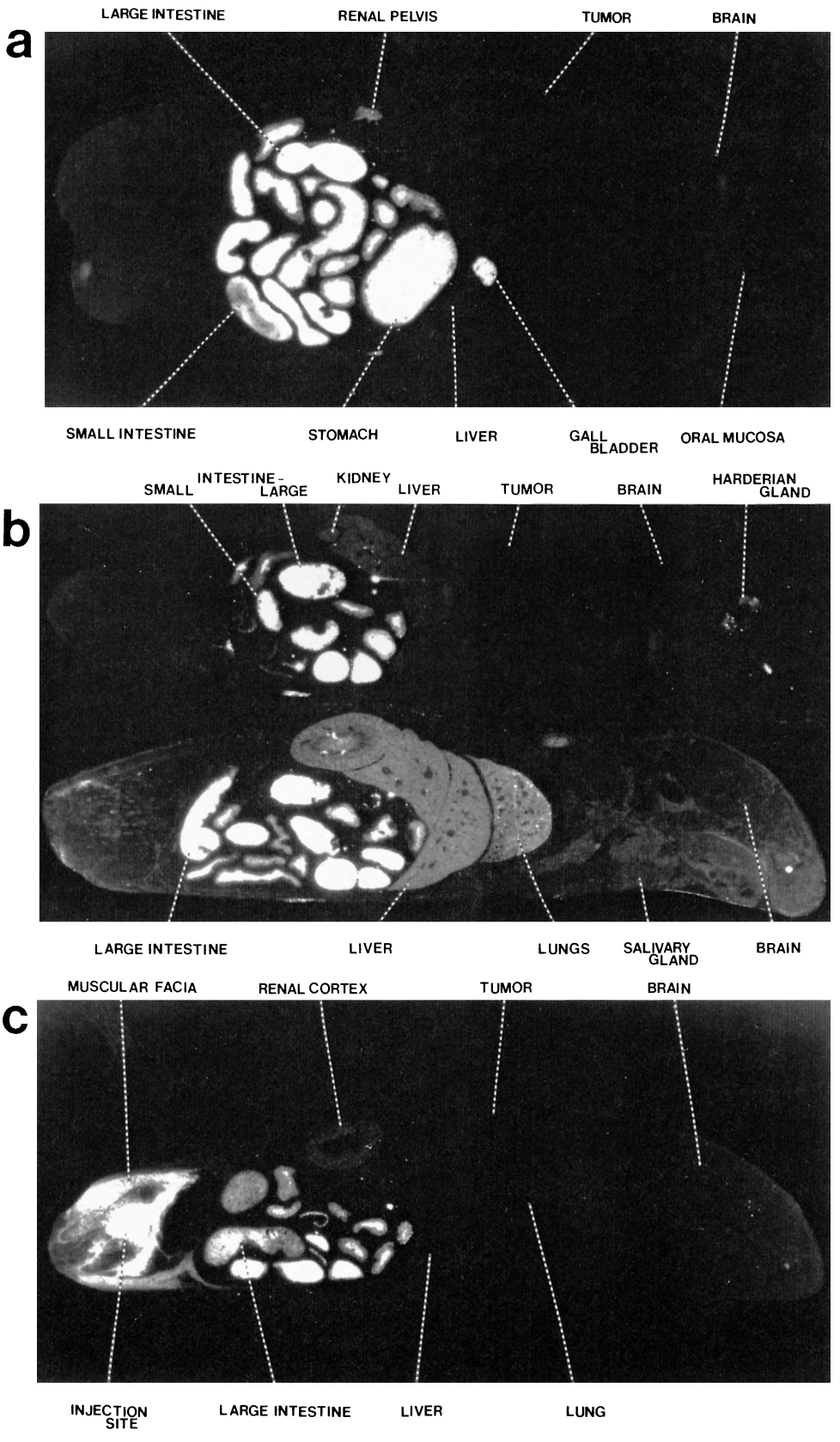


**Fig. 2 a–c** Whole body autoradiograms of mice at 2 h following (**a**) oral, (**b**) i.v. and (**c**) i.m. administration of [$^3$H]-CPT (300 μCi/kg). Note the levels of radioactivity in the stomach, intestinal contents and the gallbladder

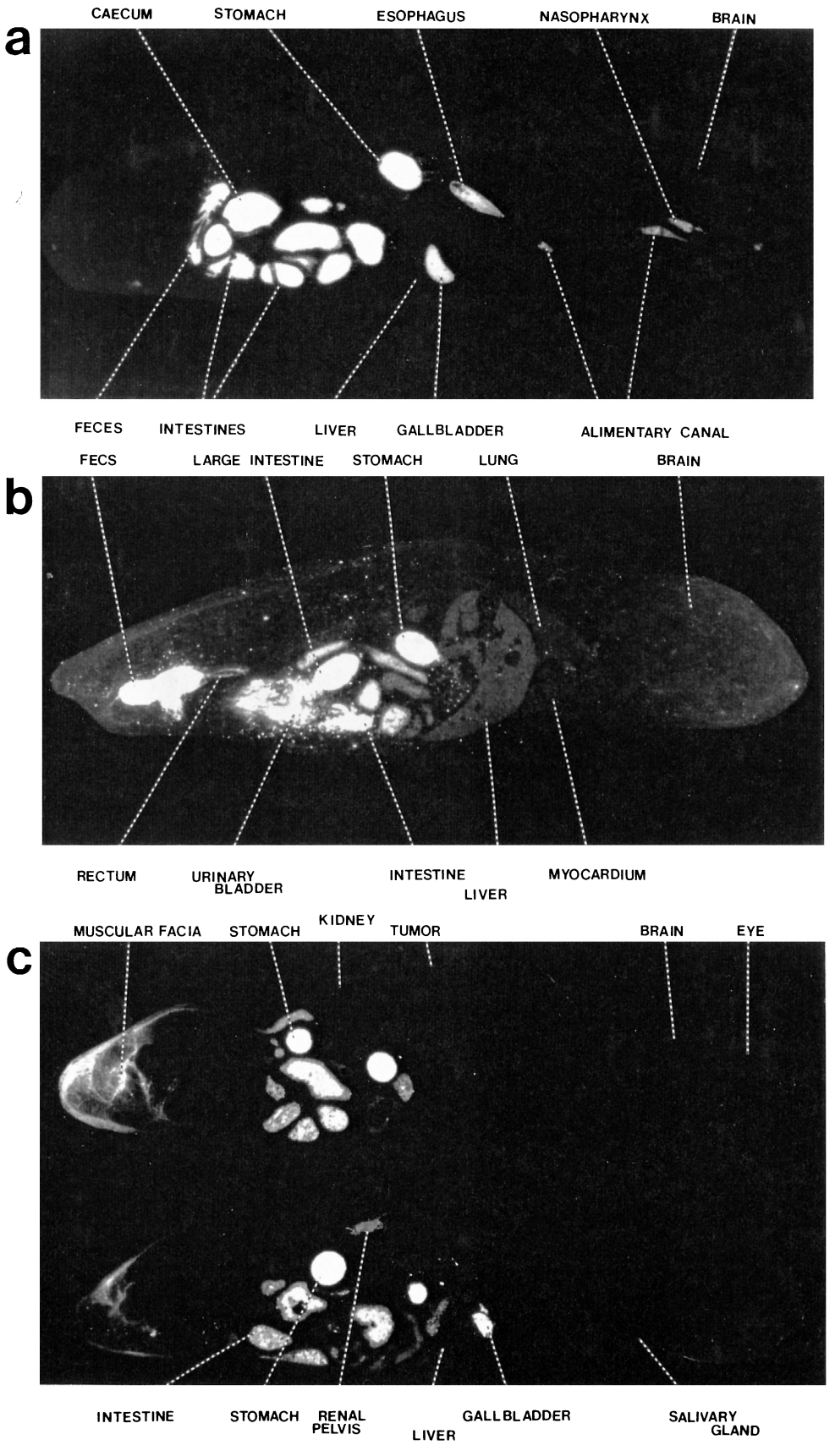


**Fig. 3 a–c** Whole body autoradiograms of mice at 12 h following (**a**) oral, (**b**) i.v. and (**c**) i.m. administration of [$^3$H]-CPT (300 μCi/kg). The retention of radioactivity in the gastrointestinal contents, liver and gallbladder is apparent. Note the delayed accumulation of [$^3$H] in the lung of i.v.-treated mice (**b**)

Tumor uptake ratios

The uptake of [$^3$H]-CPT in tumor tissues compared to other tissues and blood was determined by a method described by Fand et al. [8]. A ratio was derived from the mean of (a) lowest densitometric values obtained corresponding to tumor regions with low or absent growth and radioactivity accumulation and (b) highest densitometric values obtained corresponding to tumor regions with a high proliferation rate and the most intense radioactivity accumulation.

## Results

### Levels of radioactivity in plasma, urine and feces following [$^3$H]-CPT

Levels of radioactivity in plasma, urine, and feces of mice treated with [$^3$H]-CPT by various routes of administration are shown in Fig. 4. Initially, plasma levels of radioactivity were highest in mice treated i.v. with [$^3$H]-CPT, intermediate in mice treated i.m., and lowest in mice treated orally (Fig. 4a). At later time-points, however, levels of radioactivity derived from [$^3$H]-CPT were similar in plasma of mice treated i.m. or i.v. and were lower after oral treatment (Fig. 4a). At 24 h after treatment, the urinary excretion of [$^3$H] -CPT was high in animals treated orally compared to the low excretion rates in mice treated i.m. and i.v. (Fig. 4b). After 48 h following treatment, the urinary excretion of radioactivity was very low, independent of the route of administration. Fecal excretion of radioactivity was similar following all routes of treatment (Fig. 4c). Excretion values were high initially and decreased rapidly with time.

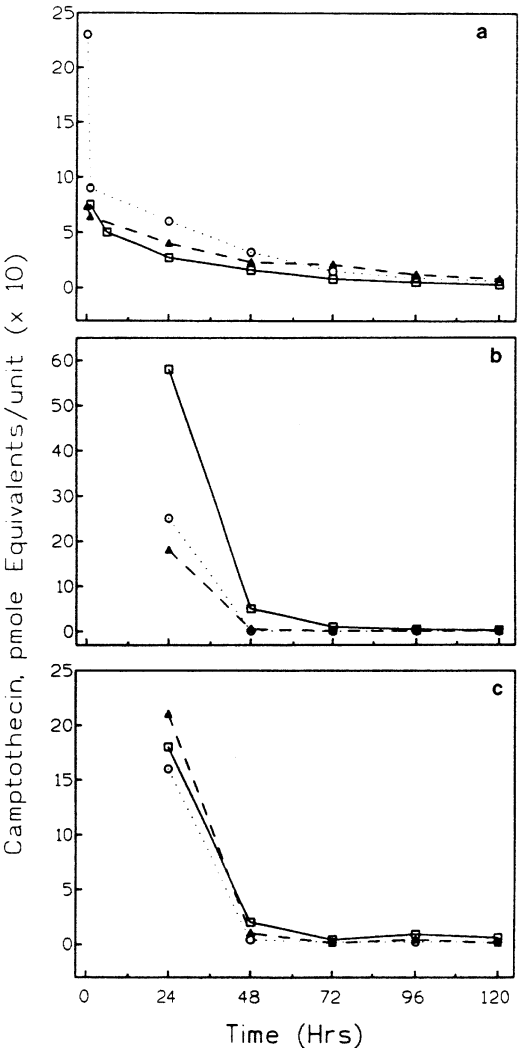


**Fig. 4 a–c** Levels of radioactivity at various time-points in (**a**) plasma faces (ml), (**b**) urine (ml), and (**c**) feces (mg) of mice treated orally (□), i.m. (▲) and i.v. (○) with [$^3$H] -CPT (300 μCi/kg)

### Distribution of radiolabel following oral, i.m. or i.v. administration of [$^3$H]-CPT

The distributions of radioactivity derived from [$^3$H]-CPT at various time-points are shown in Figs. 1–3. Irrespective of the route of administration, high levels of radioactivity were observed in the gastrointestinal contents and gallbladder 30 min after the administration of the drug (Fig. 1). Lower levels of radioactivity were observed in the liver, kidney and Harderian glands. A similar pattern of distribution but at lower [$^3$H] levels continued at 2 h (Fig. 2) and 12 h (Fig. 3), especially in the above-mentioned tissues. Irrespective of the route of administration, the localization of the radiolabel in the tumor tissues was higher in the peripheral tumor tissues than in the central area. Brain and spinal cord contained the least radioactivity in all experimental conditions.

The major difference with respect to route of administration was the higher uptake in the gastric contents, esophagus and oral mucosa of mice treated orally with the drug. The animals which had received an i.v. dose of CPT showed higher radioactivity in the lung – bronchioles than those treated by the oral and i.m. routes. Another difference observed with respect to the route of administration was the accumulation of [$^3$H] in the muscular fascia at the site of i.m. injection. These differences was directly related to the route of administration rather than to indirect or metabolic effects.

The WBA distribution of [$^3$H]-CPT was further substantiated by computer-assisted image analysis of the autoradiographs (Table 1) and by scintillation counting of tissue aliquots (data not shown). Differences observed included the higher uptake of radioactivity in the intestinal contents following i.v. and i.m. rather than following oral administration of [$^3$H]-CPT. Also the elimination of radioactivity from the gallbladder of orally treated animals was slower than that following i.m. or i.v. administration. The animals which received an i.m. dose of the drug retained more radioactivity in the blood up to 2 h. At 12 h, the

**Table 1** Time course of radioactivity (nCi/g tissue) in organs of mice as determined by computer-assisted image analysis following a single oral, i.v. or i.m. dose (4 mg/kg) of [$^3$H]-CPT (*n.i.* organ not identified in the sections analyzed). Values are means ± SD of at least 16 autoradiograms selected from two mice

| | 30 min | | | 2 h | | | 12 h | | |
|---|---|---|---|---|---|---|---|---|---|
| Organ | Oral | i.v. | i.m. | Oral | i.v. | i.m. | Oral | i.v. | i.m. |
| Heart-blood | 2.9 ± 1.7 | 1.7 ± 0.3 | 4.5 ± 2.3 | 0.4 ± 0.2 | 1.4 ± 0.2 | 10.8 ± 2.2 | 0.4 ± 0.1 | 0.9 ± 0.2 | 0.7 ± 0.3 |
| Bone marrow | 3.5 ± 1.1 | 1.0 ± 0.3 | 2.4 ± 0.4 | 0.3 ± 0.1 | 1.6 ± 0.8 | 5.1 ± 1.9 | 0.3 ± 0.1 | 0.4 ± 0.1 | 0.6 ± 0.2 |
| Tumor-cortex | 2.9 ± 0.8 | 2.7 ± 0.4 | 3.9 ± 1.1 | 0.6 ± 0.1 | 4.8 ± 0.3 | 4.3 ± 1.7 | 0.6 ± 0.1 | 0.8 ± 0.2 | 0.9 ± 0.2 |
| Tumor-pelvis | 1.8 ± 0.3 | n.i. | 2.4 ± 0.4 | 0.3 ± 0.1 | 3.7 ± 1.2 | n.i. | 0.3 ± 0.1 | n.i. | 0.5 ± 0.1 |
| Brain | 2.8 ± 0.4 | 0.9 ± 0.3 | 2.0 ± 0.3 | 0.2 ± 0.1 | 0.3 ± 0.1 | 5.6 ± 1.9 | 0.2 ± 0.1 | 0.5 ± 0.2 | 0.5 ± 0.2 |
| Harderian gland | 4.6 ± 0.8 | 2.9 ± 0.3 | 4.6 ± 2.1 | 0.5 ± 0.1 | 6.4 ± 2.6 | 17.8 ± 3.1 | 0.5 ± 0.1 | 1.7 ± 0.3 | 0.7 ± 0.1 |
| Lung | 3.2 ± 1.7 | 2.4 ± 0.2 | 3.3 ± 1.6 | 0.4 ± 0.1 | 2.7 ± 0.3 | 12.8 ± 3.1 | 0.4 ± 0.1 | 0.9 ± 0.1 | 0.6 ± 0.1 |
| Renal pelvis | 18.3 ± 6.1 | 8.2 ± 2.1 | 13.2 ± 5.2 | 15.8 ± 3.2 | 11.0 ± 3.2 | 22.1 ± 0.3 | 1.0 ± 0.2 | 2.2 ± 0.4 | 2.0 ± 0.2 |
| Liver | 10.3 ± 3.3 | 3.8 ± 0.6 | 7.9 ± 2.4 | 1.6 ± 0.2 | 4.1 ± 2.2 | 8.9 ± 2.1 | 1.9 ± 0.2 | 0.8 ± 0.3 | 1.8 ± 0.3 |
| Gallbladder | 89.8 ± 7.9 | 80.8 ± 18.0 | 120.3 ± 14.8 | 87.3 ± 17.5 | 81.8 ± 8.5 | 81.5 ± 12.3 | 69.8 ± 3.3 | 12.9 ± 0.1 | 49.9 ± 0.7 |
| Stomach contents | 101.1 ± 7.8 | 10.1 ± 2.8 | 38.7 ± 9.3 | 96.5 ± 9.2 | 45.6 ± 12.3 | 25.0 ± 9.2 | 93.3 ± 8.2 | 23.2 ± 9.8 | 43.2 ± 3.8 |
| Stomach mucosa | 15.5 ± 5.3 | 6.1 ± 2.0 | 5.0 ± 0.5 | 9.7 ± 2.4 | 7.1 ± 0.9 | 8.2 ± 1.3 | 20.7 ± 9.6 | 5.2 ± 1.3 | 4.2 ± 0.9 |
| [s]Intestinal contents | 47.5 ± 16.0 | 86.1 ± 12.2 | 95.8 ± 13.6 | 89.1 ± 14.8 | 43.8 ± 18.3 | 75.1 ± 12.0 | 85.7 ± 9.2 | 11.0 ± 3.0 | 31.0 ± 2.0 |
| [s]Intestinal mucosa | 8.9 ± 6.0 | 25.2 ± 8.1 | 32.7 ± 12.0 | 13.3 ± 3.5 | 6.3 ± 1.0 | 19.7 ± 3.5 | 19.7 ± 8.8 | 3.0 ± 1.4 | 4.2 ± 0.9 |
| [l]Intestinal contents | 18.1 ± 2.2 | 28.8 ± 13.2 | 37.5 ± 9.5 | 30.1 ± 2.2 | 16.3 ± 7.9 | 36.7 ± 11.3 | 86.3 ± 18.8 | 3.4 ± 1.0 | 6.4 ± 0.5 |
| [l]Intestinal mucosa | 6.1 ± 2.1 | 12.6 ± 4.0 | 13.8 ± 5.2 | 9.8 ± 2.2 | 5.9 ± 4.0 | 0.9 ± 2.1 | 1.8 ± 2.2 | 1.8 ± 0.3 | 2.6 ± 0.3 |

[s]Smal, [l]Large

**Table 2** Tumor/nontumor ratios derived from computer-assisted image analysis following the administration of [$^3$H]-CPT (4 mg/kg, equivalent to 300 μCi/Kg) to mice. Values are means ± SD of at least 12 determinations

| | Oral | | | i.v. | | | i.m. | | |
|---|---|---|---|---|---|---|---|---|---|
| | 30 min | 2 h | 12 h | 30 min | 2 h | 12 h | 30 min | 2 h | 12 h |
| Tumor[a]/blood | 1.01 | 1.5 | 1.5 | 1.58 | 1.57 | 0.89 | 0.07 | 0.39 | 1.28 |
| Tumor/bone marrow | 0.82 | 2.0 | 0.75 | 2.70 | 1.37 | 2.0 | 1.60 | 1.19 | 1.50 |
| Tumor/lung | 0.89 | 1.5 | 0.85 | 1.12 | 0.81 | 0.88 | 1.18 | 0.47 | 1.50 |
| Tumor/gallbladder | 0.03 | 0.01 | 0.1 | 0.03 | 0.02 | 1.0 | 0.30 | 0.07 | 0.02 |
| Tumor/gastric contents[b] | 0.05 | 0.01 | 0.01 | 0.06 | 0.06 | 0.06 | 0.71 | 0.13 | 0.04 |
| Tumor/liver | 0.22 | 0.38 | 1.2 | 0.71 | 0.53 | 0.07 | 0.39 | 0.68 | 0.75 |
| Tumor/brain | 1.03 | 3.0 | 6.0 | 3.00 | 7.33 | 1.6 | 1.90 | 1.09 | 1.80 |

[a] Tumor values are the mean of the peripheral and central zones of tumor tissues
[b] Values of gastric contents include stomach, and small and large intestines

radioactivity levels in blood were low irrespective of the route of administration.

### Ratios of tumor/nontumor tissues

The radioactivity contents of tumor tissues compared to nontumor tissues were quantitated for all experimental time-points (Table 2). The ratios demonstrate that gastric and gallbladder contents had higher levels of radioactivity than the tumor tissues. Most other tissues, however, contained less [$^3$H]-CPT-derived radioactivity than the tumor tissues. At all time-points, the concentration of radiolabel in the tumor was higher than that in the blood following oral treatment. In mice which had received an i.m. dose of [$^3$H]-CPT, the tumor/blood ratio was less than unity at 0.5 and 2 h, but had increased significantly by 12 h after treatment. At all experimental time-points, tumor/brain ratios were high irrespective of route of administration.

## Discussion

As illustrated by WBA and image analysis data, high levels of radioactivity were detected in the urinary bladder and gallbladder, intestinal tract and fecal matter of animals irrespective of treatment route. This pattern of tissue distribution was confirmed by parallel scintillation counting of tissue aliquots (data not shown). Stability studies indicate that in biological systems in vivo and in vitro, [$^3$H]-CPT is stable with a half-life of 16.5 h [17]. Thus, the majority of the radioactivity detected by autoradiography in our studies must have been in the form of [$^3$H]-CPT or its metabolites.

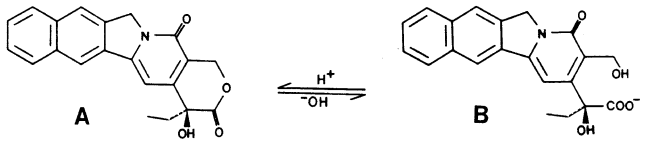


**Fig. 5** pH-dependent equilibrium of CPT in aqueous solution: (*A*) lactone and (*B*) salt forms

CPT is known to exist in an equilibrium between the lactone form (A) and salt form (B) (Fig. 5). Depending on the pH of the aqueous medium, one or the other form of CPT predominates. Thus, an orally administered dose likely exists almost entirely in the lactone form within the stomach (pH 1–2). Because of the higher lipid solubility of the lactone from compared to that of the salt, partial absorption of the lactone by passive diffusion from the stomach will occur. The remainder of the dose will pass to the duodenal portion of the small intestine (pH $\sim$ 8) , where it likely is ionized to the salt form. Thus, the drug will be trapped in the intestinal tract and most probably will be extensively eliminated via the feces, as indicated by the current study.

Following systemic administration (i.v. and i.m.), CPT likely equilibrates in the blood between the lactone and the salt forms depending on various biological factors [5, 21]. Studies in human plasma and blood have demonstrated that human serum albumin binds to the carboxylate salt form of CPT with higher affinity than to the lactone form resulting in the conversion of CPT to the salt form [21]. In contrast, the stability of CPT lactone is enhanced by its binding to erythrocyte membranes [5]. Thus, pH, albumin, erythrocytes and possibly other factors determine the stability of the CPT lactone in the circulation [5, 21]. Because of the lipid solubility of the lactone and the high molecular weight of the compound, biliary elimination from the liver is expected to predominate and to result in the observed high accumulation of CPT in the gallbladder as compared to the liver. Our results are in agreement with these physicochemical and biological properties of CPT. Independent of the route of administration, the majority of the dose was eliminated into the bile and was then accumulated in the intestinal contents. The high pH of the intestinal contents likely favored the conversion of the drug into the hydrophilic salt form, thus minimizing its reabsorption.

The uptake of [$^3$H]-CPT by tumor tissues was qualitatively similar independent of the route of administration of the drug. Quantitative determinations of radioactivity within the tumor tissues showed that the peripheral, proliferating tumor cells contained higher levels of radioactivity than central and necrotic zones. The outer zones had a granular distribution of radioactivity associated with their intact cellular structure. The central portions of the tumor consisting of areas of necrotic cells and stromal connective tissues had a homogeneous, low radioactivity level. Factors that may have influenced the uptake of CPT by the tumor tissues are the accessibility of the circulating lactone to the tumor cells and the proximity of blood vessels in the tumor periphery [8].

When tumor/blood ratios were determined using tumor regions with the highest grain densities, the localization indices exceeded those achieved by using traditional mean tissue counting data. These data suggest that tumor size and the corresponding ratio of viable to necrotic cells influenced the accretion of CPT in the tumor tissues. The tumor/blood ratio was higher than unity 30 min following i.v. or oral administration (1.5 and 1.6, respectively), was 1.5 at 2 h and then declined in mice treated i.v. In contrast, it remained high for mice treated orally. This finding suggests that the oral route is more effective pharmacologically. The tumor tissues contained low levels of radioactivity compared to gallbladder and intestinal contents. These data suggest that relatively low concentrations of the drug in tumor tissue suffice to induce the pharmacologic activity indicated by the known chemotherapeutic activity of CPT in tumor-bearing mice [12, 13].

This study also indicates that after 12 h most of the drug was eliminated from most organs except from the gastrointestinal tissues irrespective of the route of administration. Retention of the drug was observed also at the site of i.m. administration. Moreover, the gastrointestinal contents seemed to retain radioactivity for long time periods, as shown by the accumulation of [$^3$H] in stomach and intestinal contents. Thus, the retained drug at the site of i.m. injection or in the gastrointestinal system may act as a reservoir for the slow release of CPT into the circulation.

In conclusion, our experiments have shown that the gastrointestinal tract is the main site of accumulation of CPT and/or its metabolites. The consistently high tumor/blood ratios following oral administration of [$^3$H] -CPT suggest that this may be the therapeutically most effective route of treatment.

## References

1. Abbot BJ (1976) Bioassay of plant extracts for anticancer activity. Cancer Treat Rep 60:1007
2. Ahmed AE, Jacob S, Loh JP (1991) Studies on the mechanism of haloacetonitrile toxicity; quantitative whole body autoradiographic distribution of 2- [$^{14}$C] -chloroacetonitrile in rats. Toxicology 67:279–302
3. Ahmed AE, Jacob S, Au WW (1994) Quantitative whole body autoradiographic disposition of glycol ether in mice: effect of route of administration. Fundam Appl Pharmacol 22:266
4. Beck WT, Danks MK (1991) Mechanisms of resistance to drugs that inhibit DNA topoisomerases. Semin Cancer Biol 2:235–244
5. Burke TG, Mi Z (1993) Preferential binding of the carboxylate form of camptothecin by human serum albumin. Anal Biochem 212:285–287

6. D'Arpa P, Liu LF (1989) Topoisomerase-targeting antitumor drugs. Biochem Biophys Acta 989 : 163–177
7. DeWys WD, Humphreys SR, Goldin A (1968) Studies on the therapeutic effectiveness of drugs with tumor weight and survival time indices of Walker 256 carcinosarcoma. Cancer Chemother Rep 52 : 229
8. Fand I, Sharkey RM, McNally WP, Brill AB, Som P, Yamamoto K, Primus FJ, Goldenberg DM (1986) Quantitative whole-body autoradiography of radiolabeled antibody distribution in a xenografted human cancer model. Cancer Res 46 : 271
9. Gallo RC, Whang-Peng J, Adamson RH (1971) Studies on the antitumor activity mechanism of action and cell cycle effects. J Natl Cancer Inst 46 : 789
10. Giovanella BC, Stehlin JS (1973) Heterotransplantation of human malignant tumors in "nude" thymusless mice. I. Breeding and maintenance of "nude" mice. J Natl Cancer Inst 51 : 615
11. Giovanella BC, Stehlin JS, Shepard RC, Williams LJ (1983) Correlation between response to chemotherapy of human tumors in patients and in nude mice. Cancer 52 : 1146
12. Giovanella BC, Stehlin JS, Wall ME, Wani MC, Nicholas AW, Liu LF, Silber R, Potmesil M (1989) DNA topoisomerase I targeted chemotherapy of human colon cancer in xenografts. Science 246 : 1046
13. Giovanella BC, Hinz HR, Kozielski AJ, Stehlin JS, Silber R, Potmesil M (1991) Complete growth inhibition of human cancer xenografts in nude mice by treatment with 20(S) camptothecin. Cancer Res 51 : 3052
14. Gottleib JA, Guarino AM, Call JB, Olivero VT, Block JB (1970) Preliminary pharmacologic and clinical evaluation of camptothecin sodium (NSC-100880). Cancer Chem Rep 54 : (6) 461–470
15. Govindachari TR, Viswanathan N (1972) 9-Methoxy camptothecin. A new alkaloid from *Mappia foetida* Miers. Indian J Chem 10 : 453
16. Guarino AM, Andeson JB, Starkweather JA, Chignell CF (1973) Pharmacologic studies of camptothecin (NSC-100880). Distribution, plasma protein binding and biliary excretion. Cancer Chemother Rep 57 : (2) 125–140
17. Hintz HR, Harris NJ, Giovanelli BC, Ezell EL, Liehr JG (1996) Stabilities of $^{3}H$ and $^{2}H$-labeled camptothecins. J Labeled Compounds Radiopharmaceuticals 38: (8)
18. Leibovitz A, Stinson JC, McCombs III WB, McCoy LE, Mazur VC, Mabry ND (1976) Classification of human colorectal adenocarcinoma cell lines. Cancer Res 36 : 4562
19. Liu LF, D'Arpa, P (1992) Topoisomerase-targeting antitumor drugs. Mechanisms of cytotoxicity and resistance In : De Vita VT, Hellman S, Rosenberg SA (eds) Important advances in oncology, J.P. Lippincott Co., Philadelphia, pp 79–89
20. Loh JP, Ahmed AE (1990) Determination of camptothecin in biological fluids using reversed-phase high-performance liquid chromatography with fluorescence detection. J Chromatogr 530 : 367–376
21. Mi Z, Burke TG (1994) Differential interactions of camptothecin lactone and carboxylate forms with human blood components. Biochemistry 33 : 10325–10336
22. Schaeppi U, Fleishman RW, Cooney DA (1974) Toxicity of camptothecin (NSC-100880). Cancer Chem Rep 5 : 25–36
23. Scott, DO, Binra DS, Sutton SC, Stella VJ (1994) Urinary and biliary disposition of the lactone and carboxylate forms of 20 (S) camptothecin in rats. Drug Metab Dispos 22 : 438–442
24. Supko JG, Malspeis L (1993) Pharmacokinetics of the 9-amino and 10, 11-methyledioxy derivatives of camptothecin in mice. Cancer Res 53 : 3062–3069
25. Tafur S, Nelson JD, DeLong DC, Svoboda GH (1976) Anti-viral components of *Ophiiorrhiza Mungos* isolation of campothecin and 10-methoxy-camptothecin. Lloydia 39 : 261
26. Ullberg S (1977) The technique of whole-body autoradiography. Cryosectioning of large specimens (special issue on whole-body autoradiography). Science Tools, the LKB Instrument Journal, Uppsala, Sweden
27. Venditti JM, Abbot BJ (1967) Studies on oncolytic agents from natural sources. Correlations of activity against animal tumors and clinical effectiveness. Lloydia 30 : 332
28. Wall ME, Wani MC, Cook CE, Palmar KH, McPhail AT, Sim GA (1966) Plant antitumor agents I. The isolation and structure of camptothecin a novel alkaloidial leukemia and tumor inhibitor from *Camptotheca acuminata*. J Am Chem Soc 88 : 3888